

Timing and climatic impact of Greenland interstadials recorded in stalagmites from northern Turkey

D. Fleitmann,^{1,2} H. Cheng,³ S. Badertscher,^{1,2} R. L. Edwards,³ M. Mudelsee,⁴ O. M. Göktürk,^{1,2} A. Fankhauser,¹ R. Pickering,¹ C. C. Raible,^{2,5} A. Matter,¹ J. Kramers,¹ and O. Tüysüz⁶

Received 14 July 2009; revised 17 August 2009; accepted 19 August 2009; published 6 October 2009.

[1] A 50 kyr-long exceptionally well-dated and highly resolved stalagmite oxygen ($\delta^{18}\text{O}$) and carbon ($\delta^{13}\text{C}$) isotope record from Sofular Cave in northwestern Turkey helps to further improve the dating of Greenland Interstadials (GI) 1, and 3–12. Timing of most GI in the Sofular record is consistent within ± 10 to 300 years with the “iconic” Hulu Cave record. Larger divergences (>500 years) between Sofular and Hulu are only observed for GI 4 and 7. The Sofular record differs from the most recent NGRIP chronology by up to several centuries, whereas age offsets do not increase systematically with depth. The Sofular record also reveals a rapid and sensitive climate and ecosystem response in the eastern Mediterranean to GI, whereas a phase lag of ~ 100 years between climate and full ecosystem response is evident. Finally, results of spectral analyses of the Sofular isotope records do not support a 1,470-year pacing of GI. **Citation:** Fleitmann, D., et al. (2009), Timing and climatic impact of Greenland interstadials recorded in stalagmites from northern Turkey, *Geophys. Res. Lett.*, 36, L19707, doi:10.1029/2009GL040050.

1. Introduction

[2] The last glacial period is marked by rapid variations in climate termed Greenland interstadials (GI; also known as Dansgaard-Oeschger events). While the spatial extent and climatic impact of GI is well documented [Voelker, 2002], uncertainties with respect to their absolute timing exist. Uranium-series dated (^{230}Th) stalagmites [Wang et al., 2001; Genty et al., 2003; Burns et al., 2003; Wang et al., 2006; Spötl et al., 2006] have been used to develop a more coherent and absolute chronology of GI. To date, the Hulu Cave stalagmite oxygen isotope record captures GI 1–21 in detail, though its resolution is rather coarse (50–200 years) and spacing of ^{230}Th dates averages 1,600 years [Wang et al., 2001]. Other stalagmite records covering this period are discontinuous or do not show well-expressed GI in their isotopic profiles [e.g., Genty et al., 2003] (Figure 1). Additional

^{230}Th -dated stalagmites are thus required for further validation and, if necessary, refinement of the Hulu record. This is of paramount importance as the Hulu time series is being used as a ‘reference record’ for other paleoclimate records [e.g., Svensson et al., 2008; Skinner, 2008], and even to constrain radiocarbon calibration [Weninger and Joris, 2008; Hughen et al., 2006]. Here we present a 50 kyr-long stalagmite oxygen ($\delta^{18}\text{O}$) and carbon ($\delta^{13}\text{C}$) isotope record from Sofular Cave located at the Black Sea in northwestern Turkey (Figure 1 and auxiliary material Text S1).⁷ A set of 98 ^{230}Th dates with very small errors of ~ 0.25 –2.5% and highly resolved (~ 20 year resolution) $\delta^{18}\text{O}$ and $\delta^{13}\text{C}$ profiles allow us to assign precise ages to GI 1 (Bølling-Allerød (BA)), and 3–13.

[3] Furthermore, the Sofular time series fills a large spatial gap of precisely-dated, highly-resolved and long terrestrial paleoclimate records in the northeastern Mediterranean, and provides unambiguous evidence for the climatic and environmental impact of GI in this area, where current key-paleoclimate time series, such as the Lago Grande di Monticchio, and Soreq Cave records from Southern Italy and Israel respectively [Allen et al., 1999; Bar-Matthews et al., 2003], do not show a well developed GI (Figure 1).

2. Cave Location and Modern Climatology

[4] Sofular ($41^{\circ}25'\text{N}$, $31^{\circ}56'\text{E}$; So-1 and So-2) and Ovacik caves ($41^{\circ}46'\text{N}$, $32^{\circ}02'\text{E}$; O-1) are located in northwestern Turkey. Precipitation in this region averages $\sim 1,200$ mm yr^{-1} , with $\sim 75\%$ occurring between September and April (Figures S1 and S2). Moisture originates mainly from the Black Sea and, to lesser extent, from the Mediterranean and Marmara Sea. Climate in northwestern Turkey is strongly tied to the North Atlantic realm and representative for the northeastern part of the Mediterranean (Text S1 and Figure S3). Vegetation above both caves is marginally affected by human activity and consists of trees, shrubs and, to a lesser extent, grass (Figure S4).

3. Methods and Sample Description

[5] Three large active stalagmites, ranging between 1–1.75 m in height, were collected from Sofular Cave (stalagmites So-1 and So-2) and Ovacik Cave (stalagmite O-1). A total of 121 ^{230}Th dates and 5,485 stable isotope measurements were performed, although the main focus was on stalagmite So-1.

¹Institute of Geological Sciences, University of Bern, Bern, Switzerland.

²Oeschger Centre for Climate Change Research, University of Bern, Bern, Switzerland.

³Department of Geology and Geophysics, University of Minnesota-Twin Cities, Minneapolis, Minnesota, USA.

⁴Climate Risk Analysis, Hannover, Germany.

⁵Climate and Environmental Physics, Physics Institute, University of Bern, Bern, Switzerland.

⁶Eurasia Institute of Earth Sciences, Istanbul Technical University, Istanbul, Turkey.

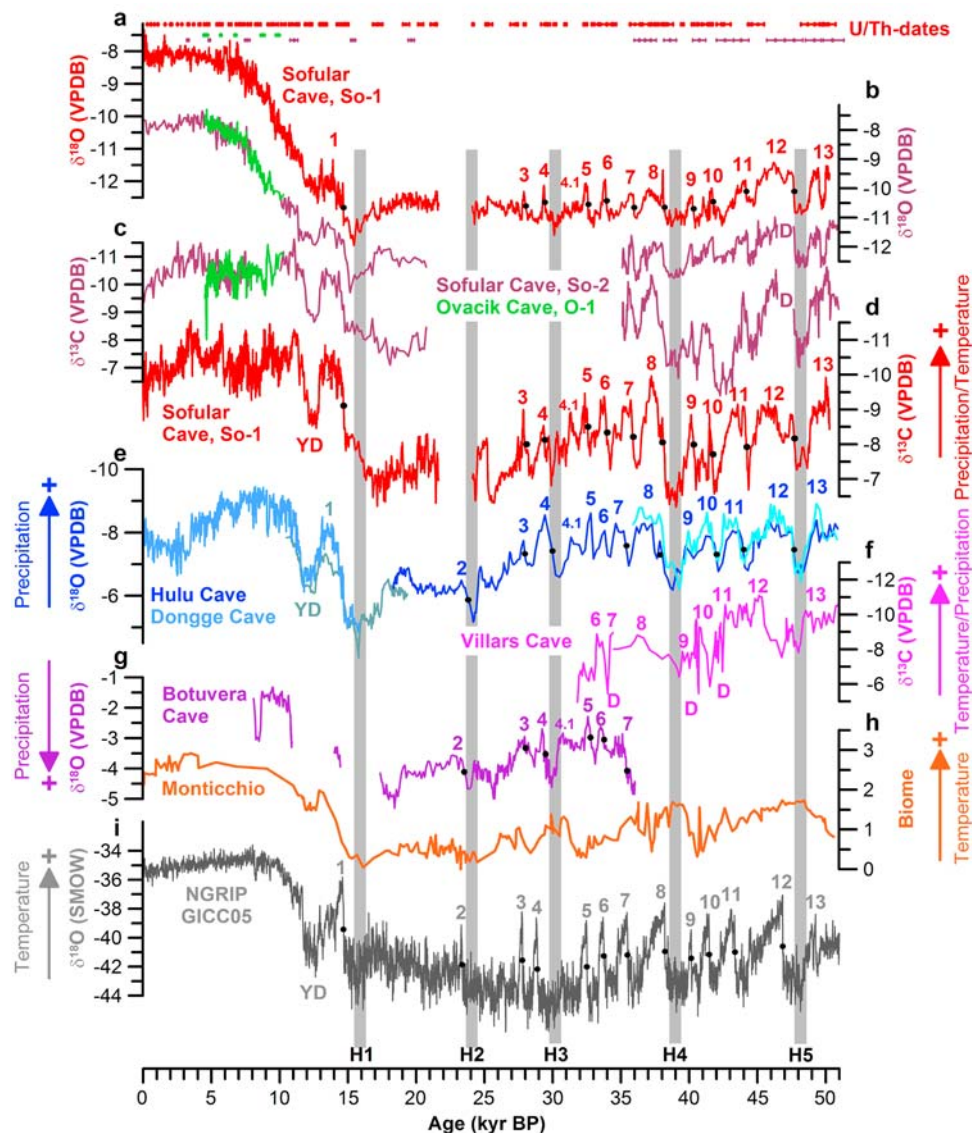


Figure 1. (a–d) The $\delta^{18}\text{O}$ and $\delta^{13}\text{C}$ time series of stalagmites So-1 and So-2 from Sofular Cave and O-1 from Ovacik Cave. Color-coded points with error bars denote ^{230}Th dates. (e) Hulu and Dongge caves records from China [Wang *et al.*, 2001; Dykoski *et al.*, 2005]. (f) Villars Cave $\delta^{13}\text{C}$ record, southwestern France [Genty *et al.*, 2003]. (g) Botuvera Cave $\delta^{18}\text{O}$ record, Brazil [Wang *et al.*, 2006]. (h) Pollen record from Lago Grande di Monticchio from southern Italy [Allen *et al.*, 1999]. (i) NGRIP $\delta^{18}\text{O}$ -profile from Greenland [Svensson *et al.*, 2008]. Numbers denote GI. Grey shaded bars denote Heinrich (H) events 1–5 [Bond *et al.*, 1993]. Letter D in the Sofular (So-2) and Villars Cave isotope profiles denote discontinuities.

[6] ^{230}Th dating of stalagmite So-1 was made on a multi-collector inductively coupled plasma mass spectrometer (MC-ICP-MS, Thermo-Finnigan-Neptune) at the Minnesota Isotope Laboratory, University of Minnesota (Table S1). Further ^{230}Th dating on all stalagmites was done on a Nu Instruments[®] MC-ICP-MS at the Geological Institute, University of Bern (Table S2). Detailed information on analytical procedures is provided in Texts S2 and S3 accompanying this article.

[7] Stable isotope analyses were performed on a Finnigan Delta V Advantage mass spectrometer equipped with an automated carbonate preparation system (Gas Bench-II) at the Institute of Geological Sciences, University of Bern. Precision of $\delta^{13}\text{C}$ and $\delta^{18}\text{O}$ measurements is 0.06‰ and 0.07‰ (1 σ -error) respectively.

[8] Uranium concentrations of ~ 0.5 ppm and low common thorium (^{232}Th) result in especially precise ^{230}Th ages for So-1; almost all of them are in stratigraphic order (Figure S5). Age models of stalagmites So-1 and O-1 are based on linear interpolation between ^{230}Th dates. Chronology of So-2 was adjusted within age uncertainties to the more precisely dated stalagmite So-1, which grew nearly continuously over the last 50.3 kyr before present (BP, “present” is defined as 1950 AD), except of a hiatus between 21.2 and 24.8 kyr BP.

4. Interpretation of Stable Isotope Profiles

[9] Isotope profiles of all stalagmites are very similar, indicating that So-1 $\delta^{18}\text{O}$ and $\delta^{13}\text{C}$ values are not biased by

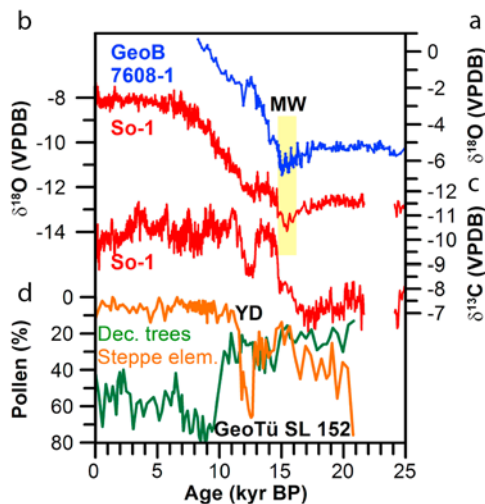


Figure 2. Comparison between Sofular Cave isotope profiles and marine sediment records from the Black and Aegean Seas. (a and b) The comparison between $\delta^{18}\text{O}$ records from the western Black Sea (GeoB 7608-1) [Bahr *et al.*, 2008] and from Sofular Cave (So-1). Yellow bar marks the interval enhanced input of isotopically depleted melt water (MW). (c and d) The comparison between the So-1 $\delta^{13}\text{C}$ time series with a pollen record from the Aegean Sea (green line = deciduous trees and orange line = steppe pollen assemblages) [Kotthoff *et al.*, 2008].

site-, cave- or sample-specific effects (e.g., kinetic fractionation effects), and furthermore that the So-1 record can be used with confidence for environmental and climatic reconstructions. Interpretation of the So-1 $\delta^{18}\text{O}$ record is not simple as $\delta^{18}\text{O}$ can be influenced by various climate variables, such as variations in surface and cave air temperatures, seasonality of precipitation, storm tracks and ice volume [McDermott, 2004]. To what extent these climate-related factors influence $\delta^{18}\text{O}$ values in our stalagmites is not fully clear. However, well expressed GI in the So-1 and So-2 $\delta^{18}\text{O}$ records suggest that decadal- to centennial-scale variations of 0.5–1.5‰ in $\delta^{18}\text{O}$ relate to climate; most likely to changes in temperature and seasonality of precipitation. On longer time-scales, So-1 $\delta^{18}\text{O}$ values are primarily influenced by changes in $\delta^{18}\text{O}$ of Black Sea surface water, as revealed by the close match between So-1 and core GeoB 7608-1 from the western Black Sea [Bahr *et al.*, 2008] (Figure 2). The drop in $\delta^{18}\text{O}$ between ~16.5 and 14.8 kyr BP due to enhanced inflow of isotopically depleted melt water [Bahr *et al.*, 2008], the subdued nature of GI 1 (BA) and the continuous increase in $\delta^{18}\text{O}$ between ~15 and 7 kyr BP are features of both records. Thus, the Black Sea was the dominant source of moisture even during the late Pleistocene.

[10] Factors governing So-1 $\delta^{13}\text{C}$ values in stalagmites are the type and density of vegetation, and soil microbial activity [Baker *et al.*, 1997; Genty *et al.*, 2003]; all of these factors are primarily dependent on effective moisture and temperature. Stalagmite $\delta^{13}\text{C}$ values of -12‰ are characteristic for C_3 (trees and shrubs) and values of -6‰ for C_4 (grasses) plants above the cave [Baker *et al.*, 1997]. Generally, a warmer and wetter climate in northwestern Turkey would promote a higher proportion of C_3 plants (trees and shrubs), denser vegetation and enhanced soil productivity, leading to more

negative $\delta^{13}\text{C}$ calcite values. Thus, stalagmite $\delta^{13}\text{C}$ values are sensitive proxies for climate-driven changes of the local ecosystem. Modern stalagmite $\delta^{13}\text{C}$ values of -10‰ are in good agreement with the C_3 dominated vegetation above Sofular and Ovacik caves.

5. Ecosystem Response to GI

[11] Between 50.3 and 14.6 kyr BP So-1 $\delta^{13}\text{C}$ values of around -8‰ are indicative of more C_4 plants, lower plant density and soil microbial activity due to colder and drier climatic conditions. This observation agrees with pollen evidence for enhanced steppe (C_4 plants; Figure 2) and reduced arboreal vegetation in the central and eastern Mediterranean [Bottema, 1995; Allen *et al.*, 1999; Kotthoff *et al.*, 2008]. In the Sofular time series GI 1 and 3–13 are characterized by negative shifts of 1–3‰ in $\delta^{13}\text{C}$ within a few decades to centuries (transition times were calculated by ramp regressions) (Figure S6 and Table S3), and reveal a greater proportion of C_3 plants and higher soil productivity due to increasing temperatures and effective moisture. Such rapid changes in vegetation have been also observed in pollen assemblages from southern Italy (Figure 1h) and Greece, although identification of GI is difficult in both records [Allen *et al.*, 1999; Tzedakis *et al.*, 2002]. Combined $\delta^{18}\text{O}$ and $\delta^{13}\text{C}$ measurements hold further information on climate and ecosystem coupling at the transition into a GI. In the So-1 $\delta^{13}\text{C}$ time series, the full transition into GI takes place within 252 ± 87 years (GI 8 not included), slower compared to 121 ± 99 years in the So-1 $\delta^{18}\text{O}$ record, and 62 ± 14 years in NGRIP (values derive from the mean and standard deviation of all transitions in So-1 and NGRIP; Figure 3a and Table S3). While the onset of GI is almost simultaneous in the So-1 $\delta^{18}\text{O}$ and $\delta^{13}\text{C}$ time series, the slightly slower transition into GI in the So-1 $\delta^{13}\text{C}$ record suggests that the ecosystem reached a kind of equilibrium with climate within ~250 years, if the equilibrium was reached at all during shorter GI.

[12] Another interesting feature of So-1 is the nature of Termination I. In contrast to pollen records from the eastern Mediterranean [Bottema, 1995; Kotthoff *et al.*, 2008], the So-1 $\delta^{13}\text{C}$ record does not exhibit a time lag of several hundreds to thousands of years between climate and vegetation at the onset of the BA and early Holocene (Figure 2). Rather, the rapid decrease of So-1 $\delta^{13}\text{C}$ values at the onset of the BA (~14.6 kyr B.P.) and the Holocene (~10.5 kyr B.P.) suggest a fast re-vegetation with trees and shrubs (C_3 plants). This observation supports the presumption that parts of the Black Sea Mountains were glacial refugia for temperate trees [Leroy and Arpe, 2007], which facilitated their rapid re-advance at the onset of the BA and Holocene. Overall, the So-1 $\delta^{13}\text{C}$ time series complements and extends pollen records from the eastern Mediterranean much further back in time, and provides, due to its precise chronology and high resolution, clear evidence for a rapid ecosystem response to GI.

6. Timing of GI

[13] GI and the Younger Dryas (YD) are clearly discernable in both So-1 isotope profiles and more explicit than in the Hulu and Villars caves records (Figure 1). This is important, as the more closely Sofular resembles NGRIP [Svensson *et al.*, 2008] and GISP2 [Meese *et al.*, 1997], the

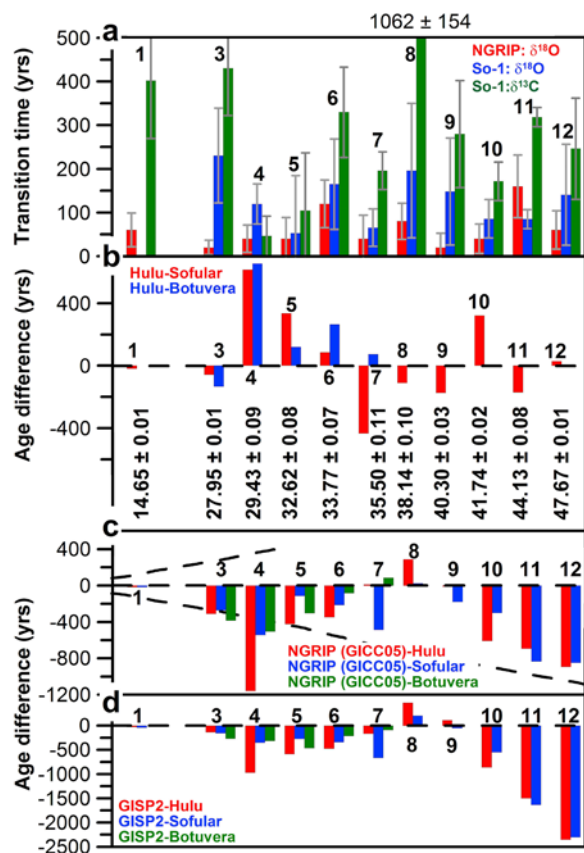


Figure 3. Transition time into GI in Sofular and NGRIP and comparison of stalagmite and ice core chronologies. Numbers denote GI. (a) Transition time into GI for NGRIP [Svensson *et al.*, 2008] and Sofular. Error bars denote ramp function uncertainties derived from bootstrap simulations (Text S4 and Table S3) [Mudelsee, 2000]. (b) Age offsets of midpoints of transitions into GI 1–13 between stalagmite chronologies from Hulu [Wang *et al.*, 2001], Sofular and Botuvera [Wang *et al.*, 2006] caves (Table S4). Numbers denote age estimates for GI based on the best fit between at least two stalagmite records. (c) Age offsets for midpoints of transitions into GI between NGRIP and Sofular and Hulu. Dashed lines denote 1σ error of the NGRIP chronology. (d) Age offsets for midpoints of transitions into GI between GISP2 [Meese *et al.*, 1997] and Sofular and Hulu.

better GI can be dated and synchronized. Midpoints of isotopic transitions into GI 1–12 (referred as midpoints hereinafter) were determined by statistical ramp function regression for the Hulu and Sofular $\delta^{18}\text{O}$ records; provided that the transition was defined by sufficiently many data points [Mudelsee, 2000] (Figures 1 and S6 and Table S4). The Villars record was not used because of its weakly expressed GI (Figure 1f). The comparison between Hulu-Sofular (Hu-So) $\delta^{18}\text{O}$ records reveals small age offsets for GI 1 ($\Delta t_{\text{Hu-So}} = -13$ yrs), 3 ($\Delta t_{\text{Hu-So}} = -75$ yrs), 5 ($\Delta t_{\text{Hu-So}} = 112$ yrs), 6 ($\Delta t_{\text{Hu-So}} = 134$ yrs), 8 ($\Delta t_{\text{Hu-So}} = -321$ yrs), 9 ($\Delta t_{\text{Hu-So}} = -166$ yrs), 10 ($\Delta t_{\text{Hu-So}} = 252$ yrs), 11 ($\Delta t_{\text{Hu-So}} = -195$ yrs) and 12 ($\Delta t_{\text{Hu-So}} = -9$ yrs), all of them are within dating uncertainties (Figure 3b and Table S5). Higher divergences are only observed for GI 4 ($\Delta t_{\text{Hu-So}} = 524$ yrs) and 7 ($\Delta t_{\text{Hu-So}} = -554$ yrs), and likely a combination of (1) ^{230}Th

dating uncertainties, (2) lower temporal resolution of Hulu, and (3) errors introduced by age model construction. In Hulu GI 4 is characterized by a broad peak in $\delta^{18}\text{O}$, which is in contrast to the relatively narrow nature of this event in Sofular, NGRIP and GISP2. Age estimate for the midpoint of GI 4 in the Botuvera (Bo) Cave record from Brazil [Wang *et al.*, 2006] (Figure 1g), differs also from Hulu ($\Delta t_{\text{Hu-Bo}} = 613$ yrs), but is in good agreement with Sofular ($\Delta t_{\text{So-Bo}} = 89$ yrs) (Figure 3b). However, the So-1 chronology seems to have an anomalous GI 7 timing, which is older as compared to Hulu and Botuvera (Figure 3b). Overall, the timing of most GI is broadly consistent between the Sofular, Hulu, and Botuvera caves records.

[14] Another important aspect of this study is the evaluation of the most recent NGRIP (GICC05) chronology [Svensson *et al.*, 2008]. The NGRIP-Sofular comparison shows non-systematic age offsets (Figure 3c). While age estimates for the midpoints of GI, are synchronous within stated 1σ -age uncertainties of the NGRIP GICC05 chronology, larger age differences are observed for GI 4 ($\Delta t_{\text{NGRIP-So}} = -586$ yrs), 7 ($\Delta t_{\text{NGRIP-So}} = -493$ yrs), 11 ($\Delta t_{\text{NGRIP-So}} = -839$ yrs), and 12 ($\Delta t_{\text{NGRIP-So}} = -855$ yrs) (Figure 3c). NGRIP-Hulu age offsets are similar, GI 11 ($\Delta t_{\text{NGRIP-Hu}} = -644$ yrs) and 12 ($\Delta t_{\text{NGRIP-Hu}} = -846$ yrs) seem to be too young in NGRIP (Figure 3c). Even larger discrepancies are observed between GISP2-Sofular and GISP2-Hulu (Figure 3d), particularly for GI 10 ($\Delta t_{\text{GISP2-So}} = -553$ yrs; $\Delta t_{\text{GISP2-Hu}} = -806$ yrs), 11 ($\Delta t_{\text{GISP2-So}} = 1636$ yrs; $\Delta t_{\text{GISP2-Hu}} = -1441$ yrs), and 12 ($\Delta t_{\text{GISP2-So}} = -2303$ yrs; $\Delta t_{\text{GISP2-Hu}} = -2294$ yrs). Overall, ice core chronologies seem to be consistently too young, whereas age offsets of GI between the Greenland ice cores and Hulu and Sofular do not increase systematically with depth. GI 7–9 seem to deviate from the general trend of generally younger ages in NGRIP and GISP2 relative to the cave records, though the reason for this deviation is yet unknown.

7. Conclusions

[15] Based on the best fit between absolutely dated stalagmites from Sofular, Hulu and Botuvera, a more robust chronological framework for GI 1, 3–12 can now be provided. This is one prerequisite for an improved radiocarbon age scale beyond ~ 24 kyr BP [Hughen *et al.*, 2006; Weninger and Joris, 2008], improvement of chronologies of ice core and sediment records, and determination of the pacing of GI. Whether GI follow an underlying cycle of $\sim 1,500$ years is controversially discussed [Yiou *et al.*, 1997; Rahmstorf, 2003]. Spectral analysis of the So-1 $\delta^{18}\text{O}$ and $\delta^{13}\text{C}$ time series do not show a significant peak around 1,500 years (Figure S7) and, thus, point to a rather stochastic forcing of GI [Ditlevsen *et al.*, 2005]. Finally, the Sofular Cave record shows, for the first time, unequivocal evidence for a rapid and sensitive climate and ecosystem response in the eastern Mediterranean to GI, and thus bears important climatic information for the Black Sea area which has been a stronghold for Neanderthal populations during the late Pleistocene [Finlayson, 2008].

[16] **Acknowledgments.** This work was supported by the Swiss National Science Foundation (grant PP002-110554/1 to D. F.), the U.S. National Science Foundation (ESH 0502535 to R. L. E. and H. C.), the

Gary Comer Science and Education Foundation (CP41 to R. L. E.), the NCCR Climate (to C. C. R.), and Istanbul Technical University (grant ITU-BAP-32491 to O. T.).

References

- Allen, J. R. M., et al. (1999), Rapid environmental changes in southern Europe during the last glacial period, *Nature*, **400**, 740–743, doi:10.1038/23432.
- Bahr, A., F. Lamy, H. W. Arz, C. Major, O. Kwiecien, and G. Wefer (2008), Abrupt changes of temperature and water chemistry in the late Pleistocene and early Holocene Black Sea, *Geochim. Geophys. Res.*, **9**, Q01004, doi:10.1029/2007GC001683.
- Baker, A., E. Ito, P. L. Smart, and R. F. McEwan (1997), Elevated and variable values of ^{13}C in speleothems in a British cave system, *Chem. Geol.*, **136**, 263–270, doi:10.1016/S0009-2541(96)00129-5.
- Bar-Matthews, M., A. Ayalon, M. Gilmour, A. Matthews, and C. J. Hawkesworth (2003), Sea-land oxygen isotopic relationships from planktonic foraminifera and speleothems in the eastern Mediterranean region and their implication for paleorainfall during interglacial intervals, *Geochim. Cosmochim. Acta*, **67**, 3181–3199, doi:10.1016/S0016-7037(02)01031-1.
- Bond, G., W. Broecker, S. Johnsen, J. McManus, L. Labeyrie, J. Jouzel, and G. Bonani (1993), Correlations between climate records from the Atlantic sediments and Greenland ice, *Nature*, **365**, 143–147, doi:10.1038/365143a0.
- Bottema, S. (1995), The Younger Dryas in the eastern Mediterranean, *Quat. Sci. Rev.*, **14**, 883–891, doi:10.1016/0277-3791(95)00069-0.
- Burns, S. J., D. Fleitmann, A. Matter, J. Kramers, and A. A. Al-Subbary (2003), Indian Ocean climate and an absolute chronology over Dansgaard/Oeschger events 9 to 13, *Science*, **301**, 1365–1367, doi:10.1126/science.1086227.
- Ditlevsen, P. D., M. S. Kristensen, and K. K. Andersen (2005), The recurrence time of Dansgaard-Oeschger events and limits on the possible periodic component, *J. Clim.*, **18**, 2594–2603, doi:10.1175/JCLI3437.1.
- Dykoski, C. A., et al. (2005), A high-resolution, absolute-dated Holocene and deglacial Asian monsoon record from Dongge Cave, China, *Earth Planet. Sci. Lett.*, **233**, 71–86, doi:10.1016/j.epsl.2005.01.036.
- Finlayson, C. (2008), On the importance of coastal areas in the survival of Neanderthal populations during the late Pleistocene, *Quat. Sci. Rev.*, **27**, 2246–2252, doi:10.1016/j.quascirev.2008.08.033.
- Genty, D., D. Blamart, R. Ouahdi, M. Gilmour, A. Baker, J. Jouzel, and S. Van-Exter (2003), Precise dating of Dansgaard-Oeschger climate oscillations in western Europe from stalagmite data, *Nature*, **421**, 833–837, doi:10.1038/nature01391.
- Hughen, K., J. Southon, S. Lehman, C. Bertrand, and J. Turnbull (2006), Marine-derived ^{14}C calibration and activity record for the past 50000 years updated from the Cariaco Basin, *Quat. Sci. Rev.*, **25**, 3216–3227, doi:10.1016/j.quascirev.2006.03.014.
- Kotthoff, U., U. C. Muller, J. Pross, G. Schmiedl, I. T. Lawson, and H. Schulz (2008), Lateglacial and Holocene vegetation dynamics in the Aegean region: An integrated view based on pollen data from marine and terrestrial archives, *Holocene*, **18**, 1019–1032, doi:10.1177/0959683608095573.
- Leroy, S. A. G., and K. Arpe (2007), Glacial refugia for summer-green trees in Europe and south-west Asia as proposed by ECHAM3 time-slice atmospheric model simulations, *J. Biogeogr.*, **34**, 2115–2128, doi:10.1111/j.1365-2699.2007.01754.x.
- McDermott, F. (2004), Palaeo-climate reconstruction from stable isotope variations in speleothems: A review, *Quat. Sci. Rev.*, **23**, 901–918, doi:10.1016/j.quascirev.2003.06.021.
- Meese, D. A., A. J. Gow, R. B. Alley, G. A. Zielinski, P. M. Grootes, M. Ram, K. C. Taylor, P. A. Mayewski, and J. F. Bolzan (1997), The Greenland Ice Sheet Project 2 depth-age scale: Methods and results, *J. Geophys. Res.*, **102**, 26,411–26,423, doi:10.1029/97JC00269.
- Mudelsee, M. (2000), Ramp function regression: A tool for quantifying climate transitions, *Comput. Geosci.*, **26**, 293–307, doi:10.1016/S0098-3004(99)00141-7.
- Rahmstorf, S. (2003), Timing of abrupt climate change: A precise clock, *Geophys. Res. Lett.*, **30**(10), 1510, doi:10.1029/2003GL017115.
- Skinner, L. C. (2008), Revisiting the absolute calibration of the Greenland ice-core age-scales, *Clim. Past Discuss.*, **4**, 295–302.
- Spötl, C., A. Mangini, and D. A. Richards (2006), Chronology and paleo-environment of Marine Isotope Stage 3 from two high-elevation speleothems, Austrian Alps, *Quat. Sci. Rev.*, **25**, 1127–1136, doi:10.1016/j.quascirev.2005.10.006.
- Svensson, A., et al. (2008), A 60 000 year Greenland stratigraphic ice core chronology, *Clim. Past Discuss.*, **4**, 47–57.
- Tzedakis, P. C., I. T. Lawson, M. R. Frogley, G. M. Hewitt, and R. C. Preece (2002), Buffered tree population changes in a Quaternary refugium: Evolutionary implications, *Science*, **297**, 2044–2047, doi:10.1126/science.1073083.
- Voelker, A. H. L. (2002), Global distribution of centennial-scale records for Marine Isotope Stage (MIS) 3: A database, *Quat. Sci. Rev.*, **21**, 1185–1212, doi:10.1016/S0277-3791(01)00139-1.
- Wang, Y. J., H. Cheng, R. L. Edwards, Z. S. An, J. Y. Wu, C. C. Shen, and J. A. Dorale (2001), A high-resolution absolute-dated late Pleistocene monsoon record from Hulu Cave, China, *Science*, **294**, 2345–2348, doi:10.1126/science.1064618.
- Wang, X. F., A. S. Auler, R. L. Edwards, H. Cheng, E. Ito, and M. Solheid (2006), Interhemispheric anti-phasing of rainfall during the last glacial period, *Quat. Sci. Rev.*, **25**, 3391–3403, doi:10.1016/j.quascirev.2006.02.009.
- Weninger, B., and O. A. Joris (2008), A ^{14}C age calibration curve for the last 60 ka: The Greenland-Hulu U/Th timescale and its impact on understanding the middle to upper Paleolithic transition in western Eurasia, *J. Hum. Evol.*, **55**, 772–781, doi:10.1016/j.jhevol.2008.08.017.
- Yiou, P., K. Fuhrer, L. D. Meeker, J. Jouzel, S. Johnsen, and P. A. Mayewski (1997), Paleoclimatic variability inferred from the spectral analysis of Greenland and Antarctic ice-core data, *J. Geophys. Res.*, **102**, 26,441–26,454, doi:10.1029/97JC00158.

S. Badertscher, A. Fankhauser, D. Fleitmann, O. M. Göktürk, J. Kramers, A. Matter, and R. Pickering, Institute of Geological Sciences, University of Bern, CH-3012 Bern, Switzerland. (fleitmanna@geo.unibe.ch)

H. Cheng and R. L. Edwards, Department of Geology and Geophysics, University of Minnesota-Twin Cities, Minneapolis, MN 55455, USA.

M. Mudelsee, Climate Risk Analysis, D-30167 Hannover, Germany.

C. C. Raible, Oeschger Centre for Climate Change Research, University of Bern, CE-3012 Bern, Switzerland.

O. Tüysüz, Eurasia Institute of Earth Sciences, Istanbul Technical University, 80626 Istanbul, Turkey.